TECTONICS, VOL. 32, 351–363, doi:10.1002/tect.20027, 2013

The role of the Zagros orogeny in slowing down Arabia-Eurasia convergence since ~5 Ma

Jacqueline Austermann[1] and Giampiero Iaffaldano[2]

Received 17 May 2012; revised 12 January 2013; accepted 3 February 2013; published 30 May 2013.

[1] Large topographic belts along convergent margins have been recognized with the ability to slowdown the kinematics of subduction over geologically short time periods (i.e., few Myr), because their associated gravitational spreading provides significant resistive force within the framework of plate tectonics. The record of past and present-day plate kinematics provides important constraints on the dynamics of the lithosphere, because plate-motion changes must reflect temporal changes in the balance of driving and resisting forces. Here we focus on the convergence between the Arabian and Eurasian plates, across the Zagros mountain belt. Relative motion across this plate boundary is reconstructed since 13 Ma from published paleomagnetic and geodetic data, and features a slowdown of ~30% from ~5 Ma to the present day. We employ global dynamic models of the mantle/lithosphere system to test whether the most recent uplift across the Arabia-Eurasia collision zone, including the Zagros orogeny, may induce the observed slowdown since 5 Ma. Specifically, we use constraints from the geologic record to infer past topography and quantify its influence on the convergence rate between Arabia and Eurasia. We test the sensitivity of our models to assumptions made in estimating the paleoelevation by perturbing the orogeny parameterization within reasonable ranges. Finally, we speculate on the potential effects of Tethys slab break-off, changes of the deformation style within the collision zone, and the Afar plume on the dynamics of convergence. Our results indicate that orogenic uplift across the Arabia-Eurasia collision zone played a key role in slowing down convergence since ~5 Ma.

Citation: Austermann, J., and G. Iaffaldano (2013), The role of the Zagros orogeny in slowing down Arabia-Eurasia convergence since ~5 Ma, *Tectonics*, *32*, 351–363, doi:10.1002/tect.20027.

1. Introduction

[2] The theory of plate tectonics [*Morgan*, 1968], proposing piece-wise motions of lithospheric plates as part of convection within Earth's mantle, relied since its birth on reconstructions of past plate kinematics inferred from the paleomagnetic record of seafloor spreading [i.e., *Gordon and Jurdy*, 1986]. Exploration of the oceans undertaken over the last two decades contributed greatly to the wealth of these records, so that today we hold information on past plate kinematics at unprecedented temporal resolution [e.g., *Müller et al*., 2008; *Torsvik et al*., 2010; *Gurnis et al*., 2012]. The advent of geodesy in Earth sciences [e.g., *Dixon*, 1991], and in particular the Global Positioning System (GPS), further augmented our knowledge by providing detailed estimates of current plate motions.

[3] Evidence is mounting from these observations that tectonic plates undergo significant kinematic changes on timescales as short as a few Myr. The principle of inertia requires that such changes must be related to temporal variations in the balance of driving and resisting forces, thus making detailed kinematic reconstructions a powerful probe into the dynamics of the lithosphere. As Earth's mantle convection evolves on much longer time scales on the order of 100 Myr to 200 Myr [e.g., *Bunge et al*., 1998], short-term plate motion changes are unlikely to be the result of variations in the pattern of mantle buoyancy forces [e.g., *Iaffaldano et al*., 2012]. More likely is the notion that geological processes occurring along plate margins induce short-term plate motion changes. For instance, reductions of the convergence rate between overriding and subducting plates have been linked to the growth of large mountain belts [e.g., *Molnar et al*., 1993; *Norabuena et al*., 1999], because the gravitational weight of their topography is capable of resisting convergence by consuming a significant amount of the driving force available to drive plate motions. *Iaffaldano et al*. [2006, 2007] and *Iaffaldano and Bunge* [2009] used geodynamic models of the mantle/lithosphere to demonstrate that large topographic features, such as the Andes of South America and the Himalayan/Tibetan system, may provide substantial resisting forces on the order of 10 TN/m along convergent margins.

[4] A prominent tectonic system that, to our best knowledge, is yet to be explored in this context is the Arabia-

[1]Department of Earth and Planetary Sciences, Harvard University, Cambridge, Massachusetts, USA.
[2]Research School of Earth Sciences, The Australian National University, Canberra, ACT, Australia.

Corresponding author: J. Austermann, Department of Earth and Planetary Sciences, Harvard University, Cambridge, MA, USA. (jaustermann@fas.harvard.edu)

0278-7407/13/10.1002/tect.20027

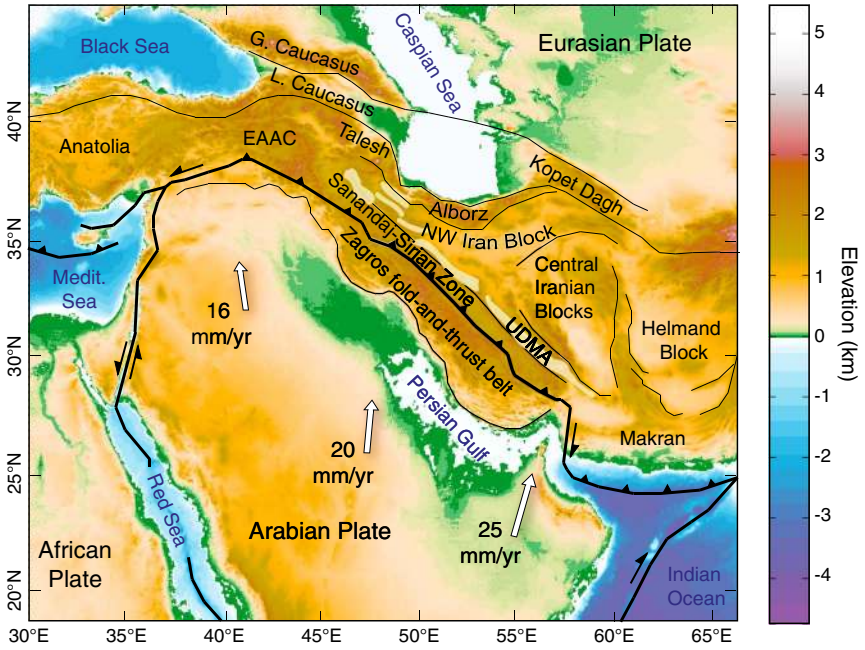

Figure 1. Tectonic setting of the Arabia-Eurasia collision zone after *Homke et al.* [2009] and *Mouthereau* [2011]. Topography is from *ETOPO2* [2001]. Velocities of Arabia with respect to Eurasia (mm/yr) are from *ArRajehi et al.* [2010]. EAAC = East Anatolian Accretionary Complex. UDMA = Urimeh-Dokhtar Magmatic Arc is denoted by transparent white regions. The thick black line denotes major plate boundaries; thin black lines denote other faults.

Eurasia collision zone (Figure 1). The active margin, where the Arabian plate converges toward Eurasia, stretches from Turkey to the western Himalayas and features elevations as high as 4500 m at the present day. The collision zone comprises the Zagros fold-and-thrust belt on the Arabian side, and a series of mountain belts and plateaus on the Eurasian side (Figure 1). The Arabia-Eurasia collision zone uplifted as part of the Alpine-Himalayan orogenic system, resulting from the subduction of the Tethys Ocean followed by large-scale continental collision. Estimates of the time of ocean closure and collision initiation range from late Cretaceous to Pliocene [*McQuarrie et al.*, 2003; *Agard et al.*, 2011, and references therein], although most studies place collision between Late Eocene and Oligocene [*Jolivet and Faccenna*, 2000; *Agard et al.*, 2005; *Vincent et al.*, 2007; *Ballato et al.*, 2011], propagating from northwest to southeast [e.g., *Agard et al.*, 2011]. In the recent geologic past, convergence between Arabia and Eurasia decreased substantially, as evident from the comparison of paleomagnetic reconstructions over the past ~3.2 Myr and geodetic measurements [*Sella et al.*, 2002; *DeMets et al.*, 2010; *Argus et al.*, 2011]. The slowdown is coeval with the proposed final uplift of the Zagros Mountains [e.g., *Allen et al.*, 2004; *Mouthereau*, 2011]. This prompted *Sella et al.* [2002] to suggest that the increasing gravitational weight of the Zagros Mountains and the Caucasus might be responsible for the slowdown of Arabia's northward convergence.

[5] Here we explore to what extent orogeny within the Arabia-Eurasia collision zone may have impacted the geologically-recent kinematics of convergence. First, we use finite rotations of the ocean-floor to reconstruct the Arabia-Eurasia convergence since ~5 Ma, when significant slowdown first initiated. We then test with global models of the coupled mantle/lithosphere system the influence of two different uplift histories on the Arabia-Eurasia convergence rate since ~5 Ma. Specifically, we compare convergence rates predicted from our models with the observed record inferred from paleomagnetic and geodetic data. Furthermore, we test the sensitivity of our models to the assumptions we make in estimating the paleoelevation of the Arabia-Eurasia collision zone at ~5 Ma. Finally, we discuss the impact of several possibly coeval events, such as the Tethys slab break-off, a change in the deformation style within the collision zone, and the presence of the Afar plume, that might have influenced the Arabia-Eurasia convergence.

2. Arabia-Eurasia Convergence Since ~5 Ma

2.1. Present-Day Convergence

[6] We obtain the present-day Euler vector for the motion of Arabia with respect to Eurasia from the geodetic estimate of *ArRajehi et al.* [2010], who employed 5 years of continuously recording GPS observations in the Kingdom of Saudi Arabia, together with new continuous GPS observations broadly distributed across the Arabian Peninsula. The Euler pole falls within the Libyan Desert (17.6 ± 0.3°E, 27.5 ± 0.1°N), with a relative rotation rate of 0.404 ± 0.004°/Myr (counter-clockwise). The inferred motion of Arabia with respect to Eurasia is a counter-clockwise rotation. Within the data precision, there is no resolvable elastic deformation of Arabia, and the resulting kinematics agree with previous geodetic estimates of *Vernant et al.* [2004] (19.5 ± 1.4°E, 27.9 ± 0.5°N, 0.41 ± 0.1°/Myr) and *McClusky et al.* [2003] (18.4 ± 2.5°E, 27.4 ± 1.0°N, 0.40 ± 0.05°/Myr). The proximity of the Euler pole to the associated Arabia-Eurasia convergent system implies a significant rotational motion of Arabia at the present day. In fact, the total convergence rate increases

from 1.65 cm/yr (at 40°E, 38°N) to 2.78 cm/yr (at 60°E, 24°N) as one moves eastward along the Arabia-Eurasia margin (Figure 2).

2.2. Past Convergence

[7] Nubia, Somalia, and Arabia were once merged into the larger African plate, before continental break-up initiated in the Afar region at about 30 Ma [*Le Pichon and Gaulier*, 1988; *Redfield et al*., 2003; *Garfunkel and Beyth*, 2006]. At the present day the boundary between Arabia and Nubia is characterized by spreading in the Red Sea, where the earliest documented magnetic anomaly (3A) occurred at ~6 Ma [*Redfield et al*., 2003; *Garfunkel and Beyth*, 2006]. Farther south, Arabia separates from Somalia in the Gulf of Aden. We reconstruct the Arabia-Eurasia relative motion since ~5 Ma from publicly available finite rotations of adjacent spreading plates composing the circuit Arabia – Nubia – North America – Eurasia. Rotation ages are constrained from the geomagnetic polarity timescale of *Cande and Kent* [1995].

[8] Several studies constrain the displacement of Arabia relative to Nubia at various times in the past from identified magnetic anomalies in the Red Sea [*Le Pichon and Gaulier*, 1988; *Jestin et al*., 1994; *Chu and Gordon*, 1998; *DeMets et al*., 2010]. Here we use the finite rotation reconstructed by *Le Pichon and Gaulier* [1988], which describes the relative

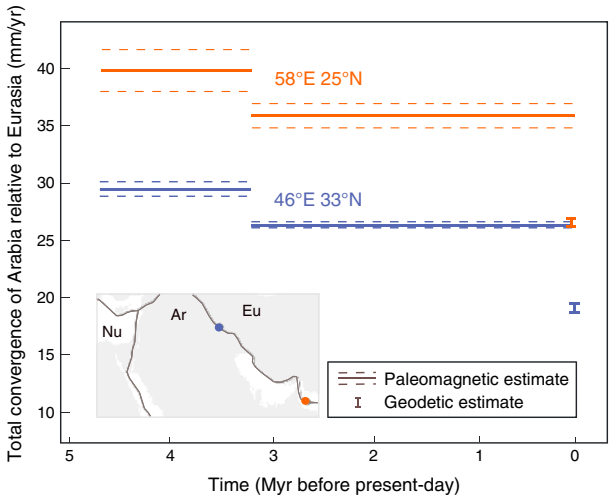

Figure 2. Arabia-Eurasia total convergence (solid lines) since ~5 Ma at 58°E 25°N (orange) and 46°E 33°N (blue—see positions in the inset), reconstructed from a selection of published finite rotations along the plate circuit Arabia – Nubia – North America – Eurasia (see section 2.2 in the main text). We compute past convergence averaged within two stages (4.7 to 3.2 Ma, and 3.2 Ma to the present day) permitted by the resolution of available finite rotations. We have verified that each component of the plate circuit contributes roughly equally to the total convergence. Error bars (dashed lines) are computed from variances of finite rotations, according to the rule of propagation of uncertainties. Present-day convergence rates and their uncertainties are obtained from geodetic estimates. Note how convergence decreases by about 1 cm/yr from ~5 Ma to the present day. Abbreviations: Ar, Arabia; Eu, Eurasia; Nu, Nubia.

Arabia-Nubia displacement accrued from ~13 Ma to the present day. Other independent studies [*Jestin et al*., 1994; *Chu and Gordon*, 1998] yield similar Euler vectors. Furthermore, we augment the temporal resolution of the Arabia-Nubia kinematics by including the relative motion since 3.2 Ma from the MORVEL kinematic model [*DeMets et al*., 2010]. Arabia-Nubia Euler poles for stages 4.7 to 3.2 Ma and 3.2 Ma to the present day are located northwest of the Red Sea, while the angular velocity decreased from 4.5 to 3.8°/Myr.

[9] The relative motion between Nubia and North America is obtained from two finite rotations reconstructed by *Müller et al*. [1999]. The associated Euler poles fall in the Arctic region and remained relatively stable since 20 Ma, while the angular velocity ranged from 2.5 to 2.7°/Myr. *McQuarrie et al*. [2003] provided an alternative reconstruction based on one single finite rotation of Nubia with respect to North America for the total relative displacement since ~20 Ma by *Klitgord and Schouten* [1986]. Although this limits the ability to resolve any plate motion variation that occurred since ~20 Ma, the reconstruction of *McQuarrie et al*. [2003] yields a similar average Euler vector as the study of *Müller et al*. [1999]. We constrain the motion of North America with respect to Eurasia from the study of *Merkouriev and DeMets* [2008], who reconstructed finite rotations since ~20 Ma at unprecedented temporal resolution. Since ~5 Ma North America-Eurasia Euler poles are located in the Antarctic region, and feature an angular velocity in range 0.2 to 0.22°/Myr.

[10] We interpolate Euler vectors from all portions on the Arabia – Nubia – North America – Eurasia circuit to obtain the Arabia-Eurasia relative motion within the stages 4.7 Ma to 3.2 Ma and 3.2 Ma to the present day. These time steps are chosen to reflect the resolution of the Arabia-Nubia record of finite rotations from MORVEL and *LePichon and Gaulier* [1988]. Uncertainties are computed according to the rule of propagation from the covariance matrices of finite rotations, when these are provided. Only for the Arabia-Nubia portion of the circuit between 4.7 and 3.2 Ma this is not the case. Having no alternative option, we assume that the uncertainty associated with the Arabia-Nubia Euler vector within this stage equals the average of the uncertainties of Nubia-North America and North America-Eurasia motions over the same stage. Our reconstructed Euler vector for the Arabia-Eurasia relative motion between 4.7 Ma and 3.2 Ma is (11°E, 32°N, 0.54°/Myr), while the Euler vector for the stage 3.2 Ma to the present day is (11°E, 34°N, 0.49°/Myr) (see Table 1 for the associated uncertainties). The magnitude of the past Euler vector is around 0.1°/Myr larger than the present-day geodetic estimate. Because the kinematic studies we employ here allow reconstructing the

Table 1. Cartesian Components of our Reconstructed Euler Vectors (ω) and Standard Deviations (σ) for Convergence of Arabia Toward Eurasia at Three Stages Since 13 Ma[a].

	Angular Velocity (°/Myr)			Standard Deviation (°/Myr)		
	ω_x	ω_y	ω_z	σ_x	σ_y	σ_z
0–3.2 Ma	0.400	0.081	0.272	0.013	0.012	0.014
3.2–4.7 Ma	0.448	0.088	0.290	0.022	0.017	0.036
4.7–13 Ma	0.437	0.087	0.255	0.044	0.025	0.056

[a]The Arabian Plate rotates with respect to Eurasia. Units are °/Myr.

Arabia-Eurasia relative motion prior to 4.7 Ma, we have verified that convergence rates were relatively stable back to at least ~13 Ma (see Euler vectors in Table 1). Our reconstruction suggests that the Arabia-Eurasia slowdown indeed must have initiated around 5 Ma.

[11] Figure 2 shows the convergence rates at two positions along the Arabia-Eurasia plate boundary, computed from geodetic and paleomagnetic estimates of Euler vectors. The present-day convergence is ~1 cm/yr slower than the long-term estimate. This difference in convergence rates since ~5 Ma occurs along the whole Arabia-Eurasia margin. Our reconstruction indicates that the motion of Arabia relative to Eurasia was characterized by a counter-clockwise rotation since at least 5 Ma, calling for a significant contribution of plate boundary forces in controlling Arabian dynamics, for otherwise its kinematics would tend to be a translation that minimizes basal mantle tractions [e.g., *Gordon*, 1998].

3. Paleoelevation at 5 Ma

[12] Does the reconstructed Arabia-Eurasia convergence slowdown result from increased resistance along the Arabia-Eurasia plate margin due to the growing topography in the Arabia-Eurasia collision zone? Addressing this question requires knowledge of the topography of this region at ~5 Ma. Significant efforts have been put into unraveling the uplift history of this region, including the use of sedimentary deposits, rates of crustal shortening, thermochronometry, fold development, and the evolution of drainage networks [*Mouthereau et al*., 2012, and references therein]. However, there is still no consensus on the uplift history.

[13] In the following, we briefly summarize the current state of knowledge on the topographic evolution, and discuss uplift histories based on two recent publications [*Allen et al*., 2004; *Mouthereau et al*., 2012]. We then use this evidence to generate two paleoelevation estimates, including an account of their uncertainties, at 5 Ma.

3.1. Constraints on the Topographic Evolution of the Arabia-Eurasia Collision Zone

[14] The youngest marine fossils from the Lake Van area on the East Anatolian High Plateau are reported to be of Serravallian age (11.5–13.6 Ma) [*Gelati*, 1975], and mark the time for uplift above sea level. The sedimentary rocks that follow these marine deposits are chiefly terrestrial conglomerates and sandstones with shales, marls, and subordinate evaporates [*Sengör et al*., 1985; *Saroglu and Yilmaz*, 1987]. The oldest volcanoes of the plateau are of the same age, but widespread uplift-related volcanism, which is linked to lithosphere delamination or slab break-off, did not commence until 7 to 6 Ma [*Pearce et al*., 1990; *Keskin et al*., 1998]. Upper Oligocene to Lower Miocene limestones are present throughout central and northern Iran due to a shallow-water epicontinental sea (Qom Formation) [*Reuter et al*., 2009]. This formation is superseded by the terrestrial Upper Red Formation, which has been dated between 17.5 and 7.5 Ma [*Ballato et al*., 2008]. These records provide a timeframe for the initiation of uplift in this area.

[15] *Ballato et al*. [2011] find that in the Alborz Mountains the transition to shallow-marine evaporates and terrestrial sediments occurred shortly after 36 Ma and marked the change-over from extension to compression. However, acceleration of regional deformation and uplift did not occur before 20–17.5 Ma. Furthermore, *Morley et al*. [2009] find that widespread crustal shortening in the Central Basin, the Zagros and the Alborz mountains occurred late (early Miocene or later) relative to the initial collision. In their study, *Ballato et al*. [2011] invoked a two-stage collision process to explain the time lag between the initiation of continental collision and the acceleration of regional deformation. Specifically, they called for a "soft" collision of stretched lithosphere at first, and "hard" collision following the arrival of unstretched Arabian continental lithosphere in the subduction zone.

[16] Most of the Zagros Folded Belt was likely close to sea-level before the most recent phase of uplift started, an inference based on the transition from the Agha Jari Formation (composed of medium-grained deltaic deposits) to the Bakhtyari Formation (which features coarse conglomerates of near-shore fan-delta deposits at the base of the section, and continental alluvial deposits at its top) [*Berberian and King*, 1981; *Homke et al*., 2004; *Fakhari et al*., 2008; *Khadivi et al*., 2010]. The timing of this transition, however, remains ambiguous and revised age constraints point to significant diachronism with a time-transgressive character from northeast to southwest [*Fakhari et al*., 2008; *Khadivi et al*., 2010]. An age range of over 20 Myr is proposed for a restored distance of only ~200 km across the Zagros [*Fakhari et al*., 2008].

[17] In addition to the constraints from the sedimentary record, we make use of the tectonic history to infer paleoelevation: Prior to collision of the Arabian Peninsula with the Eurasian continent, subduction of the Tethys ocean-floor underneath Eurasia presumably resulted in an Andean-like plate boundary. It is therefore logical to envisage that some topography along the margin on the overriding unit was already in place at the time of ocean closure. This is supported by geologic observations: Part of the Sanandaj-Sirjan Zone (SSZ) has been documented to have been an active Andean-like margin characterized by calc-alkaline magmatism [*Berberian and Berberian*, 1981] during the mid-Jurassic/Early Cretaceous. Similarly, the Urumieh-Dokhtar Magmatic Arc (UDMA) is interpreted to be a subduction-related arc that has been active since Late Jurassic [*Berberian and King*, 1981; *Berberian et al*., 1982]. The Eastern Anatolian Accretionary Complex (EAAC) in the north is located between two former subduction arcs, the Pontide and the Bitlis-Poturge [*Keskin*, 2003], which resulted from northward subduction of the Tethys oceanic lithosphere as well as of lithospheric mantle beneath the Bitlis-Poturge Massif [*Sengör et al*., 2003; *Rizaoglu et al*., 2009]. Plateau uplift has been interpreted as surface manifestation of delamination of the mantle lithosphere and/or slab break-off [*Keskin*, 2003; *Sengör et al*., 2003].

[18] Based on these findings, we assume that the SSZ, UDMA, and EAAC regions were already elevated prior to the most recent uplift phase, while everywhere else within the Arabia-Eurasia margin elevation was close to sea level, although not uniformly.

3.2. Two Proposed Uplift Histories

[19] Based on these geologic findings, two different uplift histories of the Zagros have been proposed in previous studies: *Allen et al*. [2004] argued for a discontinuous and asynchronous uplift in different regions of the Arabia-Eurasia margin, with a reorganization occurring around 5 Ma. Instead,

Mouthereau et al. [2012] suggested a more continuous and uniform uplift from 15 to 12 Ma until the present day. Because the diachronism found in the Bakhtyari conglomerates is believed to extend for only 200 km, we elect not to include it in our models. Nonetheless, we explore a range of uncertainties from different uplift histories of the Zagros folded belt.

[20] *Allen et al.* [2004] described a regional reorganization of strain at ~5 Ma, based on the observation that a number of mapped active faults would need only ~5 Myr at the current slip rates to achieve their total offset. He suggested that uplift within the Greater Caucasus, Anatolia, and the Turkish-Iranian Plateau started at ~12 Ma, but mostly ended prior to the present day. We adopt this inference, but are aware that it has been challenged by recent analyses. Specifically, shortening along the southern Greater Caucasus has been estimated to take up most of the Arabia-Eurasia convergence since ~5 Ma [*Forte et al.*, 2010], and the Greater Caucasus has experienced a major increase in exhumation since ~5 Ma [*Avdeev and Niemi*, 2011]. Instead, the outer regions—including the Zagros folded belt to the south and the Kopet Dagh, Alborz, and Lesser Caucasus to the north—started uplifting at ~7 Ma to reach their final elevation at the present day [see *Allen et al.*, 2004, Figure 7]. We therefore assume a linear uplift within the Turkish-Iranian Plateau (specifically, the regions of Anatolia, EAAC, Greater Caucasus, SSZ, NW Iran Block, UDMA, and Central Iranian Blocks in Figure 1) from 12 to 3 Ma, while uplift in the remaining regions (Zagros, Lesser Caucasus, Talesh, Alborz, Kopet Dagh, and Makran) is assumed to be continuous from 7 Ma to the present day.

[21] The alternative scenario proposed by *Mouthereau et al.* [2012] requires that we assume a linear uplift of the entire Arabia-Eurasia collision zone, starting at 12 Ma and terminating at the present day.

3.3. Inferring Paleoelevations at 5 Ma

[22] To reconstruct the paleoelevation at 5 Ma, we implement the following procedure: First, we divide the region into several subregions corresponding to plateaus or mountain chains. Next, we assign each subregion a time interval in which uplift occurred (e.g., 12 Ma to the present day) and an initial elevation prior to uplift (e.g., 200 m). The final elevation is the present-day topography of the subregion. Finally, we interpolate the topography at 5 Ma assuming that it developed linearly through time—that is, the uplift rate of each subregion remains constant through time. We consider this a reasonable choice, given the lack of more precise constraints from the published literature. The time interval for uplift is derived from the two uplift histories discussed earlier. We assume uncertainties ranging from 1 to 8 Myr for the different time intervals (see figure caption of Figure 6 for details).

[23] The initial elevation is constrained by the sedimentary deposits and the tectonic history. Based on the geologic findings discussed in section 3.1, we assume that the elevation of the SSZ, UDMA, and EAAC regions prior to the most recent uplift phase was 1000 $\pm$ 500 m, while everywhere else within the Arabia-Eurasia margin elevation was at 200 $\pm$ 100 m.

[24] Figure 3A shows the reconstructed paleoelevation assuming the asynchronous uplift history of *Allen et al.* [2004] (from here on we will refer to this as Elevation A). Note that the resolution of all the plots in Figure 3 is the same as that of the finite element grid we use in our numerical models (see section 4). Figure 3C shows the residual elevation with respect to the present day, indicating that the topographic volume uplifted since 5 Ma is ~30%, with on average 650 m increase in elevation accrued since then.

[25] Figure 3B shows the paleoelevation of the Arabia-Eurasia collision zone at 5 Ma obtained from a continuous uplift history based on *Mouthereau et al.* [2012] (from here on we will refer to this as Elevation B). The entire region is uplifted on average by 450 m since 5 Ma (Figure 3D). The two histories of uplift result in different distributions of the topographic volume accrued since 5 Ma: While the residual topography (i.e., the topography uplifted after 5 Ma) resulting from Elevation A (Figure 3C) concentrates along the Arabia-Eurasia plate margin, the one from Elevation B (Figure 3D) is more evenly distributed over the collision area.

[26] Furthermore, we generate a set of seven alternatives for both Elevation A and B by varying all input parameters (i.e. timing of uplift and initial elevation), except for the present-day elevation, within their estimated ranges of uncertainties. These alternative paleoelevations allow us to assess the sensitivity of our model results to initial assumptions (see section 5.2).

4. Global Models of the Coupled Mantle/Lithosphere System

[27] To test the impact of the reconstructed paleoelevations at 5 Ma on the Arabia-Eurasia convergence history, we resort to global models of the coupled mantle/lithosphere system. The details and capabilities of these models have been previously discussed in several studies (e.g., *Kong and Bird* [1995], *Bird* [1998, 1999], *Iaffaldano et al.* [2006, 2011], and associated supplementary information), but we provide in the following a general description.

[28] Plate velocities and their time-dependence result from the evolving balance of torques associated with forces acting upon the lithosphere. Such balance includes both shallow- and deep-rooted contributions of forces related to subducting slabs, gravitational collapse of large topographic features, friction along faults and plate boundaries, deviatoric stresses associated with lateral variations of crust and lithosphere thicknesses, and shear tractions from the convecting mantle acting at the base of tectonic plates. Over the past decades there has been much progress in developing numerical models of mantle convection on one side, and lithosphere dynamics on the other. Merging these two independent classes of models [*Iaffaldano et al.*, 2006] allows one to simulate the coupled mantle convection/plate tectonic system simultaneously accounting for key components of the torque balance.

[29] The global mantle convection code TERRA [*Bunge et al.*, 1998; *Schuberth et al.*, 2009] solves for the conservation equations of mass, momentum, and energy to compute temperature and velocity fields throughout the mantle. Local finite-elements enable achieving sufficient spatial resolution to fully resolve the dynamically important thermal boundary layers of convective motion within Earth's mantle. Furthermore, high resolution allows for strong radial variations of mantle viscosity. Here we use a viscosity of 10^{21} Pa*s for the upper mantle, increasing up to 100-fold in the lower mantle. Finally, convection models are constrained with

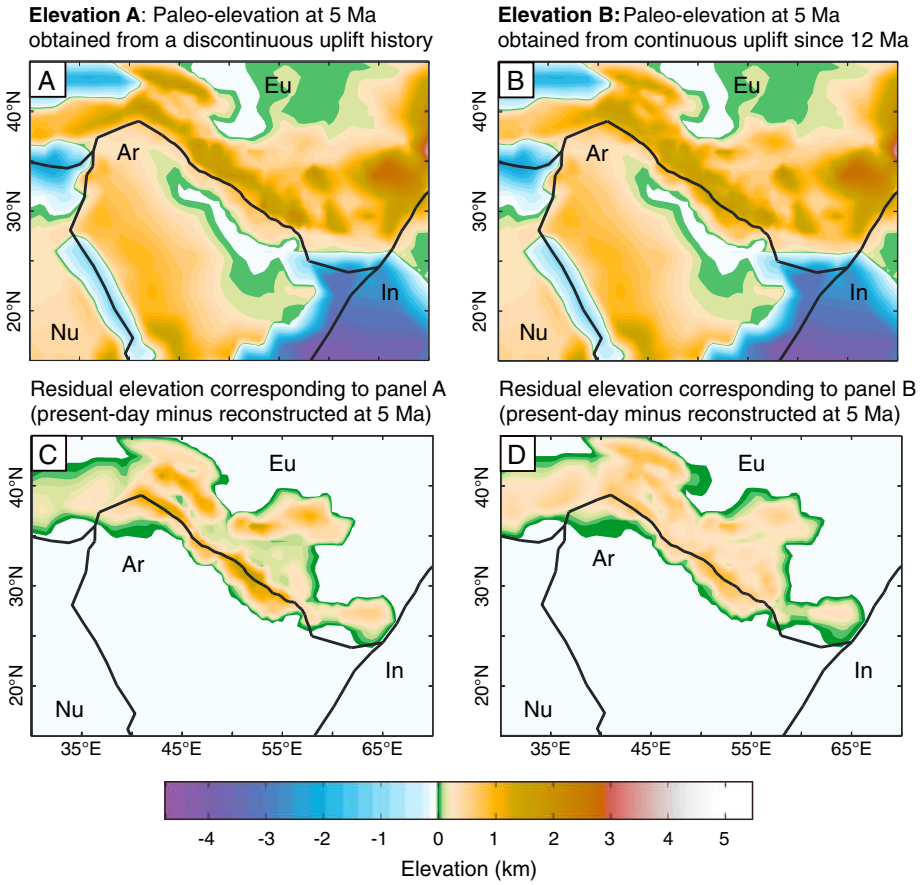

Figure 3. Estimated elevation of the wider Zagros area at 5 Ma, inferred from uplift histories proposed by (A) *Allen et al*. [2004] and (B) *Mouthereau et al*. [2012]. (C and D) The residual elevation, obtained by subtracting the elevation at 5 Ma (Figures 3A and 3B) from the present-day elevation. Elevation is plotted at the resolution of the finite element grid employed in numerical models (see Figure 4). The residual uplift is on average ~640 m for Figure 3C and ~450 m for Figure 3D. Abbreviations: Ar, Arabia; Eu, Eurasia; Nu, Nubia; In, India.

the history of surface subduction [*Lithgow-Bertelloni and Richards*, 1998] to yield global Earth's mantle flow models.

[30] The numerical model SHELLS [*Kong and Bird*, 1995] is designed to simulate global lithosphere dynamics. Based on a 2.5-D thin-shell spherical grid, it solves for the instantaneous balance of momentum to predict global plate velocities and associated force fields at equilibrium. SHELLS features a global finite-element computational grid that explicitly accounts for geological faults and plate boundaries through interfaces between finite elements [*Bird*, 1998, 1999]. Topography, heat-flow, crustal, and lithosphere thicknesses are assigned at each node based on available observations as well as estimates from isostatic balance. A vertical temperature profile at each node is also computed to define the rheological properties of the deep crust and lithosphere. Dip angles of faults and plate boundaries cast within the numerical grid are constrained from seismological observations (i.e., Wadati-Benioff planes). The rheological properties of faults and plate boundaries are accounted for by assigning weaker rheologies to selected interfaces between elements that follow realistic plate-boundary configurations. The two models are coupled by using asthenosphere velocities derived from the mantle circulation model (TERRA) as a velocity boundary condition at the base of plates in the lithosphere model (SHELLS). Plate velocities and lithosphere forces at equilibrium are the main outputs.

[31] When casting the reconstructed paleoelevations at 5 Ma into the finite-element grid (Figure 4), we implement isostatic balance to infer the paleothickness of crust and lithosphere. Doing so implies our assumption that the uplift of the Arabia-Eurasia collision zone occurred via crustal shortening and thickening. We are aware that thicknesses of crust and lithosphere would be slightly different, had elevation changes occurred as a result of mantle upwelling or lithospheric delamination. However, because these processes are not well constrained, our preference falls on making the conservative choice of implementing isostatic balance.

[32] We extend the mantle/lithosphere model by implementing the ability to include in the torque balance net slab-pulls—that is, the gravitational weight of a sinking slab reduced by the viscous resistance exerted upon it by Earth's mantle—along margins with mechanically coherent subducting slabs. In the past these forces have been estimated analytically [e.g., *Ricard et al*., 1993; *Conrad and Lithgow-Bertelloni*, 2002] from paleomagnetic reconstructions of plate subduction.

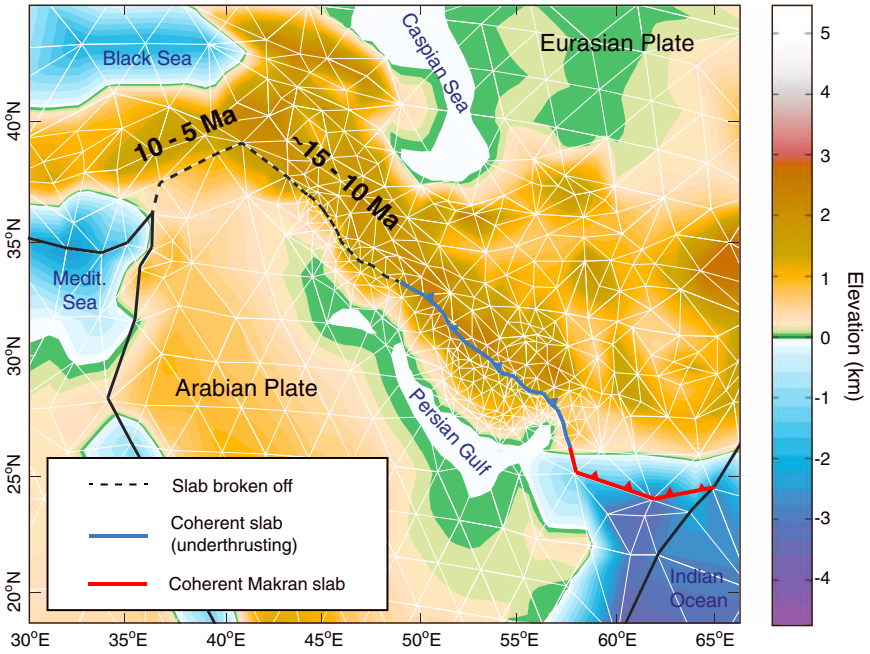

Figure 4. Finite element grid (white lines) employed in our numerical models. Elevation is plotted at the resolution of the numerical grid. Plate boundaries are in black. The boundary between Arabia and Eurasia is divided into three segments, according to the presence or absence of slabs as evident from seismic tomography [*Gorbatov and Kennett*, 2003; *Simmons et al*., 2011]. Ages indicate the suggested times of slab break-off according to *Agard et al*. [2011]. The blue and red segments show coherent slabs in tomographic images [*Simmons et al*., 2011] and have therefore slab-pull values assigned in our numerical models of mantle/lithosphere dynamics (see section 5.1 in the main text).

5. Results

5.1. Arabian Dynamics at Present Day

[33] At present day the motion of Arabia results from the influence of mantle shear tractions at the lithosphere base, gravitational spreading of the elevated Zagros, and adjacent plateaus to the northeast and the Afar/Red Sea region to the southwest, as well as the net slab-pull provided by the sinking Tethys slab along the Arabia-Eurasia margin. The contribution of mantle flow to the torque balance may be estimated from mantle circulation models, while gravitational spreading can be estimated from observations of topography. However, it is not straightforward to estimate slab-pull forces acting upon tectonic plates. The difficulty arises primarily from the challenge of accounting accurately for the density contrast between slabs and the surrounding mantle due to temperature- and pressure-induced changes of the mineral assemblages. Because the net slab-pull is the main unknown term of the present-day torque balance, we may infer its contribution in a simple inverse fashion, by requiring the Arabia-Eurasia kinematics predicted from our models to match geodetic observations of the present-day relative motion. We use seismic tomography [*Gorbatov and Kennett*, 2003; *Simmons et al*., 2011] to distinguish three main segments along the Arabia-Eurasia margin showing, to first order, different geometries and structures of the underlying mantle (Figure 4):

(1) The westernmost margin (36°E to 49°E), which shows no tomographic evidence of a slab attached to Arabia. This evidence is also supported by regional tomography studies [*Gans et al*., 2009]. Slab break-off has been suggested to have occurred under Anatolia at 10–5 Ma [*Agard et al*., 2011; *Cosentino et al*., 2012; *Schildgen et al*., 2012] and prior to 10 Ma in the northwest Zagros [*Hafkenscheid et al*., 2006; *Agard et al*., 2011].

(2) The central margin (49°E–57°E), where tomography indicates the presence of a slab dipping at a low angle and underthrusting the European lithosphere [*Simmons et al*., 2011]. This, however, is in disagreement with a proposed recent event of slab break-off in the central Zagros, inferred from the occurrence of upper Miocene-Pliocene-Quaternary adakites in the Urumieh-Dokhtar Magmatic Arc region [*Jahangiri*, 2007; *Omrani et al*., 2008]. However, there is also disagreement on the findings of *Omrani et al*. [2008] (see comment and associated reply on this paper).

(3) The easternmost Makran region (57°E–65°E), where a downgoing slab is imaged down to at least the upper mantle transition zone [*Simmons et al*., 2011].

[34] Additional evidence of the presence or absence of slabs beneath the lithosphere may come from modern seismicity and deep subduction-related earthquakes. *Engdahl et al*. [2006] assessed the seismicity in the southern Arabia-Eurasia collision zone, and identified a deep subduction zone in the Makran region. They did not report deep earthquakes along the central margin, which might indicate a shallow slab.

[35] A simple parameter search allows us to find the optimal set of net-pull values driving Arabia toward Eurasia at a rate equal to the geodetically-established one. We find 18.3 TN/m along the central segment and 1.9 TN/m along

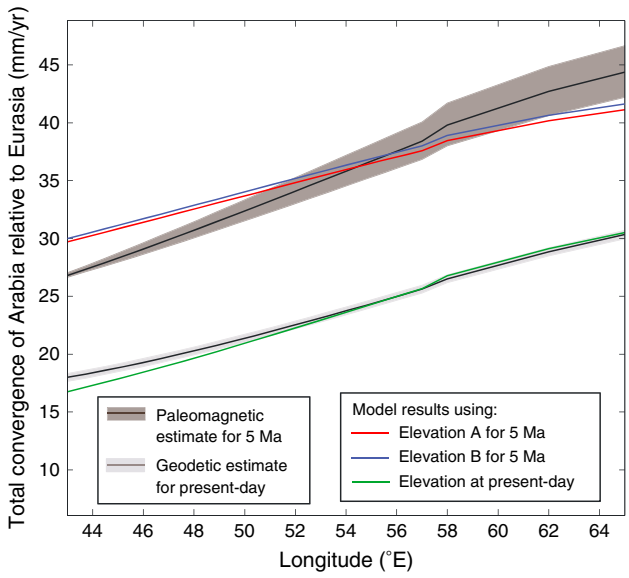

Figure 5. Reconstructed and modeled convergence rates along the Arabia-Eurasia margin. Grey lines and associated shaded areas show reconstructions from geodetic (light grey—present day) and paleomagnetic data (dark grey—~5 Ma) with their uncertainties. The green line shows model results for the present day, which are in good agreement with the geodetic estimate. The red and blue lines show model results for the Zagros paleoelevation A and B, respectively (see main text for details).

the easternmost segment. We regard this set as a reasonable estimate of the net slab-pull forces in place along the Arabia-Eurasia margin at the present day. To demonstrate the goodness of our inference, we compare in Figure 5 the present-day observed convergence rates along the Arabia-Eurasia margin (light grey line) with predictions (green line) from our models implementing the abovementioned set of net-pull forces.

5.2. Arabian Dynamics Since 5 Ma

[36] Next, we explore how uplift in the Arabia-Eurasia collision zone impacts the Arabia-Eurasia convergence in a second, distinct set of simulations. To keep our modeling assumptions as simple as possible, we set all contributions to the torque balance identical to the simulation corresponding to the present day, except for the one associated with topography in the collision zone at 5 Ma. Specifically, we modify the elevation cast into the finite-element grid within the Arabia-Eurasia margin according to the predicted paleoelevation at 5 Ma from the two different uplift histories (Figures 3A and 3B). Figure 5 shows modeled Arabia-Eurasia convergence rates across the margin in these two cases, as well as the paleomagnetic reconstruction at 5 Ma for comparison. In both cases convergence rates agree reasonably well with observations, with less than 3 mm/yr of discrepancy.

[37] Although we accounted for two different uplift histories in our models, predicted convergence rates are similar in the two cases, with Elevation B yielding slightly faster convergence rates than Elevation A. This is due to the trade-off between elevation of topography and distance from the plate boundary: on average higher topography is predicted at 5 Ma in Elevation B compared to Elevation A. One might think this leads to higher resistance at the plate boundary, and therefore slower convergence relative to the model using Elevation A. However, we point out that Elevation A features higher topography directly above the brittle portion of the plate interface than Elevation B. This implies a larger contribution to frictional shear stress as well as the horizontal deviatoric stress. It is therefore logical to expect the convergence predicted by models casting Elevation A in the finite element grid to be slightly slower than the prediction associated with Elevation B.

[38] We are aware of the assumptions we make in estimating the paleoelevation in the Arabia-Eurasia collision zone, including the initial elevation, the time of beginning and end of uplift, the linear uplift history, and the regional extent of the different mountain regions. To investigate the robustness of our conclusions, we test the sensitivity of our model to these parameters. Specifically, we generate a number of alternative paleoelevation scenarios for both uplift histories by perturbing initial elevation and timing of uplift initiation within their maximum uncertainty ranges (Figure 6). Convergence rates predicted in these cases differ from our previous models by up to 6 mm/yr. We point out that under no circumstances predicted convergence rates decrease to values comparable to the present-day ones inferred from geodetic data. This gives us confidence that our range of variability for the model paleoelevation at 5 Ma in fact captures the true, although unknown, past topography.

[39] Because the elevation along the Arabia-Eurasia margin is the only parameter varying in our models, we conclude that orogeny in the Arabia-Eurasia collision zone indeed may explain the observed 30% slowdown of Arabia-Eurasia convergence since ~5 Ma. From our models we can also estimate the contribution of orogeny to the torque balance simply as the difference of the equilibrium forces relative to the simulation corresponding to the present-day tectonic setting. We find that since 5 Ma, orogeny contributed an average resisting force of 1.8 to 1.9 TN/m along the Arabia-Eurasia plate boundary, comparable to other convergent settings worldwide [e.g., *Capitanio et al.*, 2011; *Iaffaldano et al.*, 2011].

6. Discussion

[40] A general feature of our model predictions is the less rapid increase of convergence at 5 Ma, as one moves eastward along the Arabia-Eurasia margin, compared to observations. Put simply, modeled Arabian motion at 5 Ma has a slightly smaller rotational component than observed. This is likely indicative of a coeval geologic process occurring along the convergent margin, which contributes an additional torque that is missing in our models. Figure 7 shows the misfit between the predicted convergence and the paleomagnetic estimate of convergence at 5 Ma along the plate boundary. Toward the west the predicted convergence is larger than the paleomagnetic estimate, while toward the east we find the opposite. The pole that describes the misfit is located at 24.4°N, 52.6°E, and features a magnitude of 0.16°/Myr. Could this misfit be due to an inadequate capture of the full uncertainty (i.e., covariances of finite rotations) of any part of the plate-circuit Arabia – Nubia – North America – Eurasia? Comparing the misfit

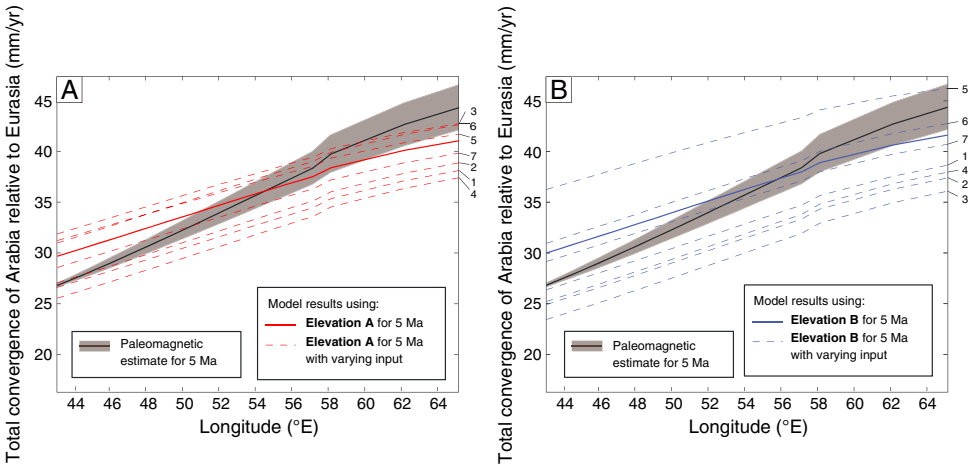

Figure 6. Reconstructed and modeled convergence rates along the Arabia-Eurasia margin. Dark grey lines and shaded areas are as in Figure 5. Red and blue lines show model results obtained by perturbing the estimates of Arabia-Eurasia collision zone paleotopography at 5 Ma. Specifically, for Elevation A (in red) we perturb the following parameters: End of uplift of the Turkish-Iranian Plateau (originally at 3 Ma), start of uplift of peripheral areas (originally at 7 Ma), initial elevation in SSZ, UDMA, and EAAC region (originally 1000 m), initial elevation in the remaining areas (originally 200 m). Perturbations are as follows: Initiation of uplift for Turkish-Iranian Plateau at 15 Ma (dashed line 1), end of uplift for Turkish-Iranian Plateau at 4 Ma (dashed line 2), start of uplift for peripheral areas at 6 Ma (dashed line 3), initial elevation in SSZ, UDMA, and EAAC region set to 1500 m (dashed line 4) and 500 m (dashed line 5), initial elevation in remaining area set to 100 m (dashed line 6) and 300 m (dashed line 7). For Elevation B (in blue) the reference parameters are: Initiation of uplift in entire region (originally at 12 Ma); initial elevation in SSZ, UDMA, and EAAC region (originally 1000 m); initial elevation in the remaining areas (originally 200 m). Perturbations are as follows: start of uplift at 15 Ma (dashed line 1), 17 Ma (dashed line 2), 20 Ma (dashed line 3), initial elevation in SSZ, UDMA, and EAAC region set to 1500 m (dashed line 4) and 500 m (dashed line 5), initial elevation in remaining area set to 100 m (dashed line 6) and 300 m (dashed line 7).

pole to the Euler Poles associated with each plate-circuit component shows that it would demonstrably require implausibly large errors on any of the finite rotations. Such misfit can therefore be interpreted in the context of a dynamic model and is a proxy for the additional, although small, torque missing in our models. Such torque must be generated by a process that increases resistance (i.e., inhibits convergence) in the west, toward Anatolia, but at the same time reduces resistance (i.e., promotes convergence) in the east, toward the Makran region. Furthermore, such mechanism is required to be active prior to 5 Ma, and to decrease thereafter. Possible candidates, which we discuss in the following sections, include slab break-off, changes of the deformation style within the collision zone, and the influence of the rising Afar plume. However, we note that temporal changes in fault dips along the margin, temporal changes in the slab pull forces due to geologic processes (e.g., underthrusting), or variations in crustal thickness due to mantle upwelling or delamination might also be potential candidates.

6.1. Slab Break-Off

[41] The break-off of the Tethys slab and the consequent variation of the net slab pull acting upon Arabia might influence the rate of convergence. Evidence for such an event is derived from the history of volcanic activity within magmatic arcs along the Arabia-Eurasia margin [*Keskin*, 2003; *Omrani et al*., 2008; *Agard et al*., 2011], and also from the geometry of mantle slabs beneath the Arabia-Eurasia margin as imaged by seismic tomography [*Hafkenscheid et al*., 2006; *Simmons et al*., 2011]. With reference to the three segments in which we divided the Arabia-Eurasia margin in Figure 4, slab break-off prior to 5 Ma has been suggested underneath Anatolia [*Keskin*, 2003; *Sengör et al*., 2003; *Cosentino et al*., 2012; *Schildgen et al*., 2012] and the North-West Zagros [*Hafkenscheid et al*., 2006; *Agard et al*., 2011]. Because plate motions readjust virtually instantaneously to changes in the torque balance, these events had no influence on the Arabian motion since 5 Ma. This argument still holds even if slab break-off had a significant time-transgressive component, as proposed by *van Hunen and Allen* [2011], as long as it occurred prior to 5 Ma.

[42] Seismic tomography [e.g., *Simmons et al*., 2011] shows the presence of a slab beneath the southeast Zagros, although it is unclear whether it is still attached to the Arabian plate. Had the slab remained mechanically coherent with the trailing plate since 5 Ma, its net-pull force at 5 Ma would have likely been smaller than its present-day value, due to the smaller slab volume and hence smaller negative buoyancy. This means that there was less pull at 5 Ma relative to the present day. Similar arguments hold true for the Makran region, furthest east along the Arabia-Eurasia boundary. However, we note that here more—rather than less—net-pull would be needed at 5 Ma to explain the mismatch (Figure 7).

[43] The change in slab pull related to break-off or ongoing subduction therefore cannot explain the pattern of spatial

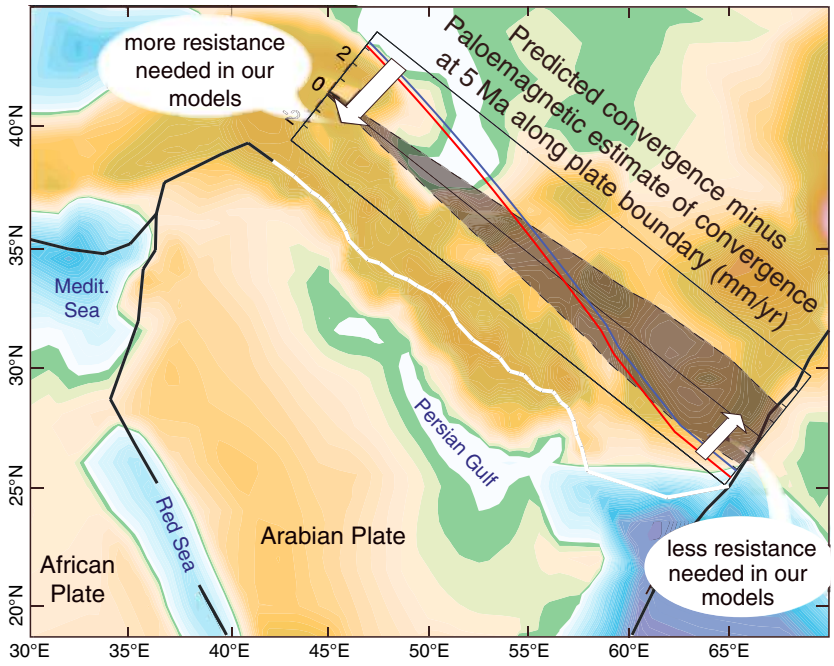

Figure 7. Misfit between predicted and observed convergence over the past 5 Ma along the Arabia-Eurasia plate boundary (white section of the otherwise black plate boundary). Colors are as in Figure 5.

variations along the Arabia-Eurasia margin. Based on this qualitative assessment, we speculate that changes in slab pull are unlikely to be among the dominant controls of Arabian dynamics since ~5 Ma.

6.2. Changes of Deformation Style Within the Collision Zone

[44] To conserve mass during convergence, collision zones uplift over time. However, they also accommodate mass via tectonic escape toward lateral regions [*Burke and Sengör*, 1986]. A notorious example is the eastward escape within the India-Eurasia collision zone [*Molnar and Tapponnier*, 1975]. *Allen et al*. [2011] proposed that the kinematic pattern on the Eurasian side of the Arabia-Eurasia collision zone changed at around 5 Ma from an eastward to a westward escape.

[45] Based on determinations of the offset for right-lateral strike-slip faults in Iran, *Allen et al*. [2011] proposed an along-strike lengthening of the Arabia-Eurasia collision zone before a change toward the present kinematic regime at ~5 Ma (Figure 8). They suggested that prior to the Afghan-India collision, the crust in Central Iran was able to deform laterally to the southeast, transferring strain into Afghanistan (Figure 8A). Once collision started, this process was no longer viable. Therefore, the escape transferred toward the north, initiating a westward transport of the South Caspian basement [*Hollingsworth et al*., 2008] and the westward escape of Anatolia (Figure 8B) [*McKenzie*, 1972]. This could also be linked to the increased exhumation and convergence rates found for the Greater Caucasus since ~5 Ma [*Avdeev and Niemi*, 2011; *Forte et al*., 2010]. This overall tectonic evolution is related to a time-transgressive closure of the Neotethys, starting in the northwest and propagating toward the southeast.

[46] How would such tectonic development affect the resistance along the plate boundary? Assuming that escape toward the East in the Makran region ceased at 5 Ma, the resistance along this part of the plate boundary would have increased toward the present day, and deformation could have been absorbed easier. Similarly, had Anatolia begun moving laterally at 5 Ma, resistance in the northwestern part of the plate boundary would have decreased toward the present day. Although such mechanism could in principle provide the additional torque that is missing in our models, it remains hard to test quantitatively, chiefly owing to the difficulties associated with modeling the temporal evolution of crustal faults and their branches in continental interiors.

6.3. Afar Plume

[47] Finally, another process occurring within the Arabian region is the opening of the Gulf of Aden and the Red Sea, followed by initiation of ocean-floor spreading. *Becker and Faccenna* [2011] suggested that at the present day the upwelling of the Afar plume is among the dominant forces controlling the northward motion of the Arabian plate. However, the events related to the opening of the Red Sea that could have potentially produced a kinematic change of the Arabian plate are documented to begin well before 5 Ma [e.g., *Ghebreab*, 1998; *Redfield et al*., 2003, and references therein]. One should therefore expect to detect their effects only in the kinematic record prior to that stage. It is plausible, nonetheless, that the upwelling of the Afar plume promoted counter-clockwise rotation that was still acting upon Arabia by 5 Ma, but decreased since then. Results from analogue models indicate that rifting is strictly connected to—and caused by—collisional processes and trench locking along the western portion of the Arabia-Eurasia plate boundary [*Bellahsen et al*., 2003]. One could

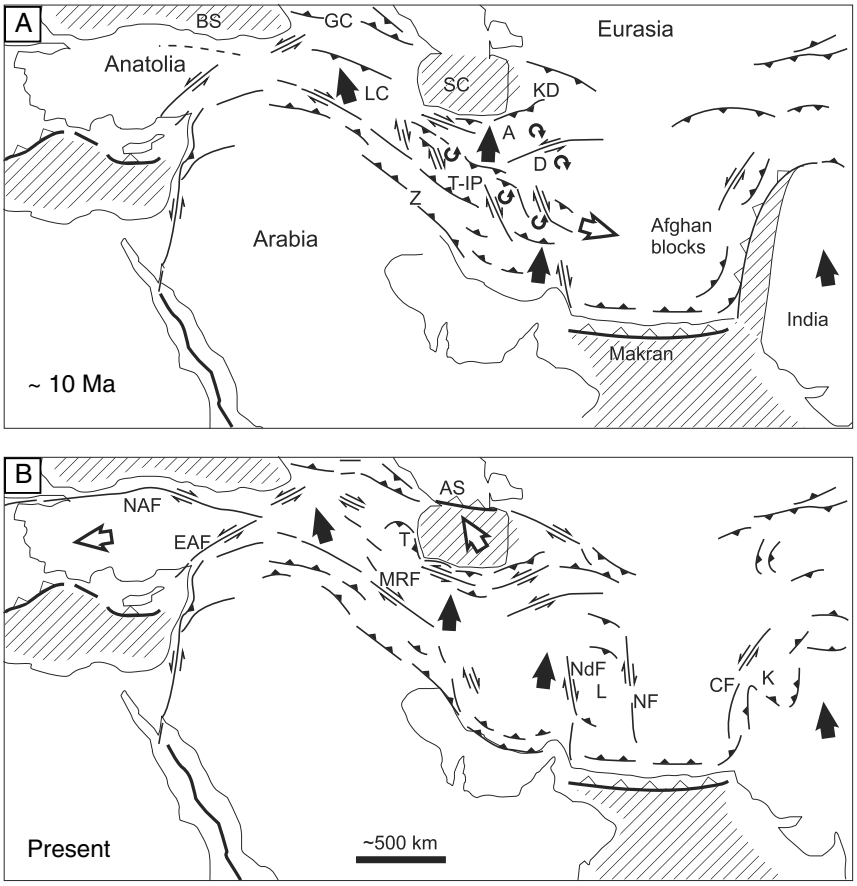

Figure 8. Sketch of the kinematics within the Arabia-Eurasia collision before (A) and after (B) the reorganization due to the collision of Afghan crust with the western margin of the Indian plate during the Pliocene. This figure is reproduced after Figure 13 in *Allen et al*. [2011]. Shaded areas are oceanic crust. Solid arrows denote motion within the collision zone with respect to stable Eurasia, adapted in (B) from the GPS-derived velocity field of *Vernant et al*. [2004] and *Reilinger et al*. [2006]. Open arrows show motion departing significantly from the overall convergence direction. Abbreviations: A, Alborz; AS, Absheron Sill; BS, Black Sea; CF, Chaman Fault; D, Doruneh Fault; EAF, East Anatolian Fault; GC, Greater Caucasus; K, Katawaz Basin; KD, Kopeh Dagh; L, Lut; LC, Lesser Caucasus; MRF, Main Recent Fault; NF, Neh Fault; NAF, North Anatolian Fault; NdF, Nayband Fault; SC, South Caspian Basin; T, Talesh; T-IP, Turkish Iranian plateau; Z, Zagros.

speculate on the interplay between plume dynamics and convergence evolution, but quantitative constraints remain sparse and prevent posing a clear testable hypothesis.

7. Conclusions

[48] We reconstructed the convergence of Arabia toward Eurasia since 13 Ma from finite rotations of the ocean-floor along the plate circuit Arabia – Nubia – North America – Eurasia. We found that convergence slowed down by ~30% from ~5 Ma to the present day. The slowdown is coeval with the proposed most recent episode of uplift of the Zagros and adjacent regions in the Arabia-Eurasia collision zone. We employed global models of the coupled mantle lithosphere system to test the extent to which orogeny in this region since ~5 Ma may have impacted the Arabia-Eurasia convergence. Specifically, we compared observed convergence rates with predictions obtained from an estimate of the Arabia-Eurasia collision zone paleoelevation at ~5 Ma, according to two histories of uplift proposed in previous studies. We found that in both cases orogeny indeed may explain the observed convergence slowdown. Furthermore, we corroborated our results by exploring the sensitivity of our models to assumptions we made in estimating the paleoelevation. Finally, we speculated about potential coeval effects that might have influenced the convergence rate along the Arabia-Eurasia plate boundary. Based on qualitative assessments, we argued that slab break-off and the Afar plume are not good candidates to explain the discrepancies between predicted and observed convergence rates. Instead, changes in the deformation pattern within the collision zone from an eastward to a westward escape may qualitatively explain the small misfit between our predictions and the paleomagnetic estimate. Our results indicate that orogenic uplift within the Zagros and adjacent regions plays a key role in slowing down convergence since ~5 Ma. The absence of any major slowdown of convergence prior to 5 Ma, despite the fact that some geologic evidence of topographic development has been gathered, suggests that other tectonic forces might have been in place to counterbalance the force associated with the topographic load.

[49] **Acknowledgments.** This study originates from a discussion with Seth Stein, and was carried out during J.A.'s visit to the Research School of Earth Sciences (RSES) at the Australian National University (ANU). We thank RSES for their support, and are grateful to B. Kennett for his advice. We thank C. DeMets, M. Allen, and an anonymous reviewer as well as the editor T. Ehlers and the associate editor J. Geismann, for their careful comments. Funding for J.A. was provided by the Klaus Murmann Fellowship of the Foundation of German Business. G.I. acknowledges support from the Ringwood Fellowship at the ANU.

References

Agard, P., J. Omrani, L. Jolivet, and F. Mouthereau (2005), Convergence history across Zagros (Iran): constraints from collisional and earlier deformation, *Int. J. Earth Sci.*, *94*, TC4025, 401–419, doi:10.1007/s00531-005-0481-4.

Agard, P., J. Omrani, L. Jolivet, H. Whitechurch, B. Vrielynck, W. Spakman, P. Monié, B. Meyer, and R. Wortel (2011), Zagros orogeny: a subduction-dominated process, *Geol. Mag.*, *148*(5–6), 692–725, doi:10.1017/S001675681100046X.

Allen, M., J. Jackson, and R. Walker (2004), Late Cenozoic reorganization of the Arabia-Eurasia collision and the comparison of short-term and longterm deformation rates, *Tectonics*, *23*, TC2008, doi:10.1029/2003TC001530.

Allen, M., M. Kheirkhah, M. H. Emami, and S. J. Jones (2011), Right-lateral shear across Iran and kinematic change in the Arabia Eurasia collision zone, *Geophys. J. Int.*, *184*, 555–574, doi:10.1111/j.1365-246X.2010.04874.x.

Argus, D. F., R. G. Gordon, and C. DeMets (2011), Geologically current motion of 56 plates relative to the no-net-rotation reference frame, *Geochem. Geophys. Geosyst.*, *12*, Q11001, doi:10.1029/2011GC003751.

ArRajehi, A., et al. (2010), Geodetic constraints on present-day motion of the Arabian plate: Implications for Red Sea and Gulf of Aden rifting, *Tectonics*, *29*, TC3011, doi:10.1029/2009TC002482.

Avdeev, B., and N. A. Niemi (2011), Rapid Pliocene exhumation of the central Greater Caucasus constrained by low-temperature thermochronometry, *Tectonics*, *30*, TC2009, doi:10.1029/2010TC002808.

Ballato, P., N. R. Nowaczyik, A. Landgraf, M. R. Strecker, A. Friedrich, and S. H. Tabatabaei (2008), Tectonic control on sedimentary facies pattern and sediment accumulation rates in the Miocene foreland basin of the southern Alborz Mountains, northern Iran, *Tectonics*, *27*, TC6001, doi:10.1029/2008TC002278.

Ballato, P., C. E. Uba, A. Landgraf, M. R. Strecker, M. Sudo, D. F. Stockli, A. Friedrich, and S. H. Tabatabaei (2011), Arabia-Eurasia continental collision: Insights from late Tertiary foreland-basin evolution in the Alborz Mountains, northern Iran, *GSA Bull.*, *123*(1/2), 106–131, doi:10.1130/B30091.1.

Becker, T. W., and C. Faccenna (2011), Mantle conveyor beneath the Tethyan collisional belt, *Earth Planet. Sci. Lett.*, *310*, 453–461, doi:10.1016/j.epsl.2011.08.021.

Bellahsen, N., C. Faccenna, F. Funiciello, J. M. Daniel, and L. Jolivet (2003), Why did Arabia separate from Africa? Insights from 3-D laboratory experiments, *Earth Planet. Sci. Lett.*, *216*, 365–381, doi:10.1016/S0012-821X(03)00516-8.

Berberian, F., and M. Berberian (1981), Tectono-plutonic episodes in Iran, in *Zagros Hindu Kush Himalaya, Geodynamic evolution*, edited by H. K. Gupta, and F. M. Delany, pp. 5–32, AGU, Washington DC.

Berberian, M., and G. C. P. King (1981), Towards a paleogeography and tectonic evolution of Iran, *Can. J. Earth Sci.*, *18*, 210–265.

Berberian, F., I. D. Muir, R. J. Pankhurst, and M. Berberian (1982), Late Cretaceous and early Miocene Andean-type plutonic activity in northern Makran and Central Iran, *J. Geol. Soc. London*, *139*, 605–614.

Bird, P. (1998), Testing hypotheses on plate-driving mechanisms with global lithosphere models including topography, thermal structure, and faults, *J. Geophys. Res.*, *103*, 10,115–10,129.

Bird, P. (1999), Thin-plate and thin-shell finite element programs for forward dynamic modeling of plate deformation and faulting, *Comput. Geosci.*, *25*, 383–394.

Bunge, H.-P., M. A. Richards, C. Lithgow-Bertelloni, J. R. Baumgardner, S. P. Grand, and B. A. Romanovicz (1998), Time scales and heterogeneous structures in geodynamic earth models, *Science*, *280*, 91–95.

Burke, K., and C. Sengör (1986), Tectonic escape in the evolution of the continental crust, *Geodyn. Series*, *14*, 41–53.

Cande, S. C., and D. V. Kent (1995), Revised calibration of the geomagnetic polarity timescale for the late cretaceous and Cenozoic, *J. Geophys. Res.*, *100*(B4), 6093–6095.

Capitanio, F., C. Faccenna, S. Zlotnik, and D. R. Stegman (2011), Subduction dynamics and the origin of Andean orogeny and the Bolivian Orocline, *Nature*, *480*, 83–86, doi:10.1038/nature10596.

Chu, D., and G. Gordon (1998), Current plate motions across the Red Sea, *Geophys. J. Int.*, *135*, 313–328.

Conrad, C. P., and C. Lithgow-Bertelloni (2002), How mantle slabs drive plate tectonics, *Science*, *298*, 207–209, doi:10.1126/science.1074161.

Cosentino, D., T. F. Schildgen, P. Cipollari, C. Faranda, E. Gliozzi, N. Hudáčková, S. Lucifora, and M. R. Strecker (2012), Late Miocene surface uplift of the southern margin of the Central Anatolian Plateau, Central Taurides, Turkey, *GSA Bull.*, *124*, 133–145, doi:10.1130/B30466.1.

DeMets, C., R. G. Gordon, and D. F. Argus (2010), Geologically current plate motions, *Geophys. J. Int.*, *181*, 1–80, doi:10.1130/B30466.1.

Dixon, T. H. (1991), An introduction to the Global Positioning System and some geological applications, *Rev. Geophys.*, *29*, 249–276.

Engdahl, E. R., J. A. Jackson, S. C. Myers, E. A. Bergman, and K. Priestley (2006), Relocation and assessment of seismicity in the Iran region, *Geophys. J. Int.*, *167*, 761–778, doi:10.1111/j.1365-246X.2006.03127.x.

ETOPO2 (2001), U.S. Department of Commerce, National Oceanic and Atmospheric Administration, National Geophysical Data Center. 2-minute Gridded Global Relief Data (ETOPO2). http://www.ngdc.noaa.gov/mgg/fliers/01mgg04.html.

Fakhari, M. D., G. J. Axen, B. K. Horton, J. Hassanzadeh, and A. Amini (2008), Revised age of proximal deposits in the Zagros foreland basin and implications for Cenozoic evolution of the High Zagros, *Tectonophys.*, *451*, 170–185, doi:10.1016/j.tecto.2007.11.064.

Forte, A. M., E. Cowgill, T. Bernardin, O. Kreylos, and B. Hamann (2010), Late Cenozoic deformation of the Kura fold-thrust belt, southern Greater Caucasus, *GSA Bull.*, *122*(3–4), 465–486, doi:10.1130/B26464.1.

Gans, C. R., S. L. Beck, G. Zandt, C. B. Biryol, and A. A. Ozacar (2009), Detecting the limit of slab break-off in central Turkey: new high-resolution *Pn* tomography results, *Geophys. J. Int.*, *179*, 1566–1572, doi:10.1111/j.1365-246X.2009.04389.x.

Garfunkel, Z., and M. Beyth (2006), Constraints on the structural development of Afar imposed by the kinematics of the major surrounding plates, in *Afar volcanic province within the East African rift system*, Vol. 259, pp. 23–42, Geological Society, London, Special Publications, doi:10.1144/GSL.SP.2006.259.01.04.

Gelati, R. (1975), Miocene marine sequence from Lake Van, eastern Turkey, *Riv. Ital. Paleont. Stratigr.*, *81*, 477–490.

Ghebreab, W. (1998), Tectonics of the Red Sea region reassessed, *Earth Sci. Rev.*, *45*, 1–44.

Gorbatov, A., and B. L. N. Kennett (2003), Joint bulk-sound and shear tomography for western Pacific subduction zones, *Earth Planet. Sci. Lett.*, *210*, 527–543, doi:10.1016/S0012-821X(03)00165-1.

Gordon, R. G. (1998), The plate tectonic approximation: Plate nonrigidity, diffuse plate boundaries, and global plate reconstructions, *Annu. Rev. Earth Planet. Sci.*, *26*, 615–642.

Gordon, R. G., and D. M. Jurdy (1986), Cenozoic global plate motions, *J. Geophys. Res.*, *91*, 12,389–12,406.

Gurnis, M., M. Turner, S. Zahirovic, L. DiCaprio, S. Spasojevic, R.-D. Müller, J. Boyden, M. Seton, V. C. Maneaa, and D. J. Bower (2012), Plate tectonic reconstructions with continuously closing plates, *Comput. Geosci.*, *38*, 35–42, doi:10.1016/j.cageo.2011.04.014.

Hafkenscheid, E., M. J. R. Wortel, and W. Spakman (2006), Subduction history of the Tethyan region derived seismic tomography and tectonic reconstructions, *J. Geophys. Res.*, *111*(B08401), doi:10.1029/2005JB003791.

Hollingsworth, J., J. Jackson, R. Walker, and H. Nazari (2008), Extrusion tectonics and subduction in the eastern South Caspian region since 10 Ma, *Geology*, *36*, 763–766, doi:10.1130/G25008A.1.

Homke, S., J. Vergés, M. Graces, H. Emami, and R. Karpuz (2004), Magnetostratipgraphy of Miocene-Pliocene Zagros foreland deposits in the front of the Pushe Kush arc, (Lurestan Province, Iran), *Earth Planet. Sci. Lett.*, *225*, 397–410, doi:10.1016/j.epsl.2004.07.002.

Homke, S., J. Vergés, J. Serra-Kiel, G. Bernaola, I. Sharp, M. Garcés, I. Montero-Verdú, R. Karpuz, and M. H. Goodarzi (2009), Late Cretaceous-Paleocene formation of the proto-Zagros foreland basin, Lurestan Province, SW Iran, *Geol. Soc. Am. Bull.*, *121*(7-8), 963–978, doi:10.1130/B26035.1.

Iaffaldano, G., and H.-P. Bunge (2009), Relating rapid plate motion variations to plate boundary forces in global coupled models of the mantle/lithosphere system: effects of topography and friction, *Tectonophys.*, *474*(1–2), 393–404, doi:10.1016/j.tecto.2008.10.035.

Iaffaldano, G., H.-P. Bunge, and T. H. Dixon (2006), Feedback between mountain belt growth and plate convergence, *Geology*, *34*, 893–896, doi:10.1130/G22661.1.

Iaffaldano, G., H.-P. Bunge, and M. Buecker (2007), Mountain belt growth inferred from histories of past plate convergence: A new tectonic inverse problem, *Earth Planet. Sci. Lett.*, *260*, 516–523, doi:10.1016/j.epsl.2007.06.006.

Iaffaldano, G., L. Husson, and H.-P. Bunge (2011), Monsoon speeds up Indian plate motion, *Earth Planet. Sci. Lett.*, *304*, 503–510, doi:10.1016/j.epsl.2011.02.026.

Iaffaldano, G., T. Bodin, and M. Sambridge (2012), Reconstructing plate-motion changes in the presence of finite-rotations noise, *Nat. Commun.*, *3*:1048, doi:10.1038/ncomms2051.

Jahangiri, A. (2007), Post-collisional Miocene adakitic volcanism in NM Iran: geochemical and geodynamic implications, *J. Asian Earth Sci.*, *30*(3–4), 433–447, doi:10.1016/j.jseaes.2006.11.008.

Jestin, F., P. Huchon, and J. M. Gaulier (1994), The Somalia plate and the East Africa Rift System: present-day kinematics, *Geophys. J. Int.*, *116*, 637–654.

Jolivet, L., and C. Faccenna (2000), Mediterranean extension and the Africa-Eurasia collision, *Tectonics*, *19*(6), 1095–1106.

Keskin, M. (2003), Magma generation by slab steepening and breakoff beneath a subduction-accretion complex: An alternative model for collision-related volcanism in Eastern Anatolia, Turkey, *Geophys. Res. Lett.*, *30*(24), 8046, doi:10.1029/2003GL018019.

Keskin, M., J. A. Pearce, and J. G. Mitchell (1998), Volcano-stratigraphy and geochemistry of collision-related volcanism on the Erzurum-Kars Plateau, North Eastern Turkey, *J. Volcanol. Geotherm. Res.*, *85*, 355–404.

Khadivi, S., F. Mouthereau, J.-C. Larrasoana, J. Vergés, O. Lacombe, E. Khademi, E. Beamud, M. Melinte-Dobrinescu, and J.-P. Suc (2010), Magnetochronology of synorogenic Miocene foreland sediments in the Fars arc of the Zagros folded belt (SW Iran), *Basin Res.*, *22*, 918–932, doi:10.1111/j.1365-2117.2009.00446.x.

Klitgord, K. D., and H. Schouten (1986), Plate kinematics of the central Atlantic, in *The Geology of North America*, edited by P. R. Vogt, and B. E. Tucholke, pp. 351–378, Geol. Soc. of Am, Boulder, Colorado.

Kong, X., and P. Bird (1995), Shells: a thin-shell program for modeling neotectonics of regional or global lithosphere with faults, *J. Geophys. Res.*, *100*, 22,129–22,131.

Le Pichon, X., and J.-M. Gaulier (1988), The rotation of Arabia and the Levant fault system, *Tectonophys.*, *153*, 271–294.

Lithgow-Bertelloni, C., and M. A. Richards (1998), Dynamics of Cenozoic and Mesozoic plate motions, *Rev. Geophys.*, *36*, 27–78.

McClusky, S., R. Reilinger, S. Mahmoud, D. B. Sari, and A. Tealeb (2003), GPS constraints on Africa (Nubia) and Arabia plate motions, *Geophys. J. Int.*, *155*, 126–138, doi:10.1046/j.1365-246X.2003.02023.x.

McKenzie, D. P. (1972), Active tectonics of the Mediterranean region, *Geophys. J. R. Astr. Soc.*, *30*, 109–185.

McQuarrie, N., J. M. Stock, C. Verdel, and B. P. Wernickek (2003), Cenozoic evolution of Neotethys and implications for the causes of plate motions, *Geophys. Res. Lett.*, *30*(20), 2036, doi:10.1029/2003GL017992.

Merkouriev, S., and C. DeMets (2008), A high-resolution model for Eurasia-North America plate kinematics since 20 Ma, *Geophys. J. Int.*, *173*, 1064–1083, doi:10.1111/j.1365-246X.2008.03761.x.

Molnar, P., and P. Tapponnier (1975), Cenozoic Tectonics of Asia: Effects of a Continental Collision, *Science*, *189*, 419–426.

Molnar, P., P. England, and J. Martinod (1993), Mantle dynamics, uplift of the Tibetan plateau, and the Indian monsoon, *Rev. Geophys.*, *31*, 357–396.

Morgan, W. J. (1968), Rises, trenches, great faults, and crustal blocks, *J. Geophys. Res.*, *73*, 1959–1982.

Morley, C. K., B. Kongwung, A. A. Julapour, M. Abdolghafourian, M. Hajian, D. Waples, J. Warren, H. Otterdoom, K. Srisuriyon, and H. Kazemi (2009), Structural development of a major late Cenozoic basin and transpressional belt in Central Iran: The central basin in the Qom-Saveh area, *Geosphere*, *5*(4), 325–362, doi:10.1130/GES00223.1.

Mouthereau, F. (2011), Timing of uplift in the Zagros belt/Iranian plateau and accommodation of late Cenozoic Arabia-Eurasia convergence, *Geol. Mag. 148*(5–6), 726–738, doi:10.1017/S0016756811000306.

Mouthereau, F., O. Lacombe, and J. Vergés (2012), Building the Zagros collisional orogen: Timing, strain distribution and the dynamics of Arabia/Eurasia plate convergence, *Tectonophys.*, *532–535*, 27–60, doi:10.1016/j.tecto.2012.01.022.

Müller, R. D., J.-Y. Royer, S. C. Cande, W. R. Roest, and S. Maschenkov (1999), New constraints on Caribbean plate tectonic evolution, in *Sedimentary Basins of the World*, vol. 4, edited by P. Mann, pp. 33–59, Elsevier, Oxford.

Müller, R. D., M. Sdrolias, C. Gaina, and W. R. Roest (2008), Age, spreading rates and spreading asymmetry of the world's ocean crust, *Geochem. Geophys. Geosyst.*, *9*, Q04006, doi:10.1029/2007GC001743.

Norabuena, E. O., T. H. Dixon, S. Stein, and C. G. A. Harrison (1999), Decelerating Nazca–South America and Nazca-Pacific plate motions, *Geophys. Res. Lett.*, *26*, 3405–3408.

Omrani, J., P. Agard, H. Whitechurch, M. Benoit, G. Prouteau, and L. Jolivet (2008), Arc-magmatism and subduction history beneath the Zagros Mountains, Iran: A new report of adakites and geodynamic consequences, *Lithos*, *106*, 380–398, doi:10.1016/j.lithos.2008.09.008.

Pearce, J. A., J. F. Bender, S. E. De Long, W. S. F. Kidd, P. J. Low, Y. Güner, F. Saroglu, Y. Yilmaz, S. Moorbath, and J. G. Mitchell (1990), Genesis of collision volcanism in Eastern Anatolia, Turkey, *J. Volcanol. Geotherm. Res.*, *44*, 189–229.

Redfield, T. F., W. H. Wheeler, and M. Often (2003), A kinematic model for the development of the Afar depression and its paleogeographic implications, *Earth Planet. Sci. Lett.*, *216*, 383–398, doi:10.1016/S0012-821X(03)00488-6.

Reilinger, R., et al. (2006), GPS constraints on continental deformation in the Africa-Arabia-Eurasia continental collision zone and implications for the dynamics of plate interactions, *J. Geophys. Res.*, *111*(B05411), doi:10.1029/2005JB004051.

Reuter, M., W. E. Piller, M. Harzhauser, O. Mandic, B. Berning, F. Roegl, A. Kroh, M.-P. Aubry, U. Wielandt-Schuster, and A. Hamedani (2009), The Oligo-/Miocene Qom Formation (Iran): evidence for an early Burdigalian restriction of the Tethyan Seaway and closure of its Iranian gateways, *Int. J. Earth Sci.*, *98*, 627–650, doi:10.1007/s00531-007-0269-9.

Ricard, Y., M. Richards, C. Lithgow-Bertelloni, and Y. Le Stunff (1993), A geodynamic model of mantle density heterogeneity, *J. Geophys. Res.*, *98*, 21,895–21,909.

Rizaoglu, T., O. Parlak, V. Höck, F. Koller, W. E. Hames, and Z. Billor (2009), Andean-type active margin formation in the eastern Taurides: Geochemical and geochronogical evidence from the baskil granitoid (Elazig, SE Turkey), *Tectonophys.*, *473*(1–2), 188–207, doi:10.1016/j.tecto.2008.08.011.

Saroglu, F., and Y. Yilmaz (1987), Geological evolution and basin models during the neotectonic episode in eastern Anatolia, *Bill. Min. Res. Expl. Inst.*, Turkey, *107*, 61–83.

Schildgen, T. F., D. Cosentino, A. Caruso, R. Buchwaldt, C. Yildirim, S. A. Bowring, B. Rojay, H. Echtler, and M. R. Strecker (2012), Surface expression of Eastern Mediterranean slab dynamics: Neogene topographic and structural evolution of the SW margin of the Central Anatolian Plateau, Turkey, *Tectonics*, *31*, TC2005, doi:10.1029/2011TC003021.

Schuberth, B. S. A., H.-P. Bunge, G. Steinle-Neumann, C. Moder, and J. Oeser (2009), Thermal versus elastic heterogeneity in high-resolution mantle circulation models with pyrolite composition: High plume excess temperatures in the lowermost mantle, *Geochem. Geophys. Geosyst.*, *10*, Q01W01, doi:10.1029/2008GC002235.

Sella, G. F., T. H. Dixon, and A. Mao (2002), Revel: A model for recent plate velocities from space geodesy, *J. Geophys. Res.*, *107*, B42081, doi:10.1029/2000JB000033.

Sengör, A. M. C., N. Gürör, and F. Saroglu (1985), Strike-slip faulting and related basin formation in zones of tectonic escape: Turkey as a case study, in *Strike-slip Deformation, Basin Formation, and Sedimentation*, edited by K. T. Biddle, and N. Christie-Blick, pp. 227–264, Soc. Econ. Paleont. Min. Spec. Pub. 37 (in honor of J. C. Crosell), Tulsa, Okla.

Sengör, A. M. C., S. Özeren, R. Genc, and E. Zor (2003), East Anatolian high plateau as a mantle-supported, north-south shortened domal structure, *Geophys. Res. Lett.*, *30*(24), 8045, doi:10.1029/2003GL017858.

Simmons, N. A., S. C. Myers, and G. Johannesson (2011), Global-scale P wave tomography optimized for prediction of teleseismic and regional travel times for Middle East events: 2. Tomographic inversion, *J. Geophys. Res.*, *116*, B04305, doi:10.1029/2010JB007969.

Torsvik, T. H., B. Steinberger, M. Gurnis, and C. Gaina (2010), Plate tectonics and the net lithosphere rotation over the past 150 My, *Earth Planet. Sci. Lett.*, *291*, 106–112, doi:10.1016/j.epsl.2009.12.055.

Van Hunen, J., and M. B. Allen (2011), Continental collision and slab break-off: A comparison of 3-D numerical models with observations, *Earth Planet. Sci. Lett.*, *302*, 27–37, doi:10.1016/j.epsl.2010.11.035.

Vernant, P., et al. (2004), Present-day crustal deformation and plate kinematics in the Middle East constrained by GPS measurements in Iran and northern Oman, *Geophys. J. Int.*, *157*, 381–398, doi:10.1111/j.1365-246X.2004.02222.x.

Vincent, S. J., A. C. Morton, A. Carter, S. Gibbs, and T. G. Barabadze (2007), Oligocene uplift of the Western Greater Caucasus: an effect of initial Arabia-Eurasia collision, *Terra Nova*, *19*, 160–166, doi:10.1111/j.1365-3121.2007.00731.x.